

## QUASI-3D MODELLING OF TWO-PHASE FLOWS IN PIPES

**Alexander VIKHANSKY**

CD-adapco, Didcot, UK

E-mail: alexander.vichansky@cd-adapco.com

### ABSTRACT

The paper demonstrated that the so-called quasi-3D (Q3D) pipe flow model can be implemented in a commercial CFD code with minimal modifications. We use a special meshing technique in order to create a two-dimensional block of control volumes stretched along the horizontal chord of the pipe so the code operating in the 3D mode effectively solves the Q3D chord-averaged Navier-Stokes equations. Turbulence is modelled by the  $k - \epsilon$  model with slightly modified coefficients.

**Keywords:** multiphase pipeline transport, free surface flow, pipe flow, quasi-3D .

### NOMENCLATURE

#### Greek Symbols

$\alpha$  Volume fraction.  
 $\epsilon$  Turbulence dissipation rate,  $[m^2/s^3]$ .  
 $\kappa$  Relative roughness.  
 $\mu_T$  Turbulent viscosity,  $[kg/ms]$ .  
 $\rho$  Mass density,  $[kg/m^3]$ .  
 $\tau$  Reynolds stress,  $[Pa]$ .  
 $\tau_s$  Particle relaxation time,  $[s]$ .

#### Latin Symbols

$A$  Cross section area,  $[m^2]$ .  
 $C_D$  Drag coefficient.  
 $C_\mu$  Turbulent viscosity prefactor.  
 $d_p$  Particle diameter,  $[m]$ .  
 $D_T$  Turbulent dispersion coefficient,

$[kg/ms]$ .  
 $F_{TD}$  Turbulent dispersion force,  $[kg/(ms)^2]$ .  
 $f$  Friction factor.  
 $\mathbf{g}$  Acceleration of gravity,  $[m/s^2]$ .  
 $\mathbf{I}$  Identity matrix.  
 $k$  Turbulence kinetic energy,  $[m^2/s^2]$ .  
 $p$  Pressure,  $[Pa]$ .  
 $Re$  Reynolds number.  
 $T_L$  Lagrangian time scale,  $[s]$ .  
 $\mathbf{u}$  Velocity,  $[m/s]$ .  
 $\bar{\mathbf{u}}$  Mean velocity,  $[m/s]$ .  
 $\mathbf{u}'$  Deviation from the mean velocity,  $[m/s]$ .

#### Sub/superscripts

$G$  Gas.  
 $L$  Liquid.  
 $S$  Solid.  
 $R$  Relative.

### INTRODUCTION

Traditionally the pipe flow simulators are based on 1D models, where the essential physics such as inter-phase drag and flow regimes are modelled using empirical correlations.

Three decades or so of intensive R&D activity in the field imply that the 1D models reach maximum of their predictive capacity. On the other hand, the growing power of modern computers allows an engineer to perform more CPU time-consuming calculations either on his own computer or on a remote server. Although the full 3D modelling of a multiphase flow in an industrial pipeline belongs to a distant future, there is a growing interest to the Q3D models where parameters of the flow are either pre-integrated across the pipe (Biberg, 2007) or averaged along the horizontal chord of the pipe (Laux *et al.*, 2007). These models allow for (an approximate) resolution of the gas-liquid interface and therefore, the transition from the stratified to bubbly flow is computed rather than modelled.

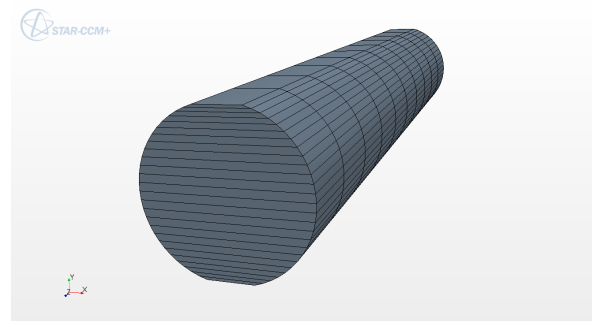


Figure 1: Q3D mesh.

Development of a dedicated Q3D software tool is an ambitious task; in the present work we demonstrate that an existing commercial 3D software can be used for the same purpose. The advantage of our approach is obvious: there are lot of physical models e.g., RANS turbulence, phase transition, VoF, which are already available for a general user. We show that the standard version of STAR-CCM+ enables one to perform transient two-phase Q3D simulations on a desktop PC within few days – an action, which would require weeks of a multiprocessor cluster if done in a full 3D mode.

### MODEL DESCRIPTION

Although our aim is to model multiphase pipe flows, the essential elements of the approach can be illustrated on a

single-phase incompressible flow. The equations for the multiphase flows are familiar for an experienced reader and can be found elsewhere.

### Pipe meshing

The Q3D mesh is shown in Figure 1. The initially circular shape of the pipe is slightly clipped from above and below in order to create a curvilinear rectangle with two horizontal edges. Then side edges are split into  $N_y$  segments and the Directed Mesh option of STAR-CCM+ is applied in order to create a two-dimensional block of prismatic cells.

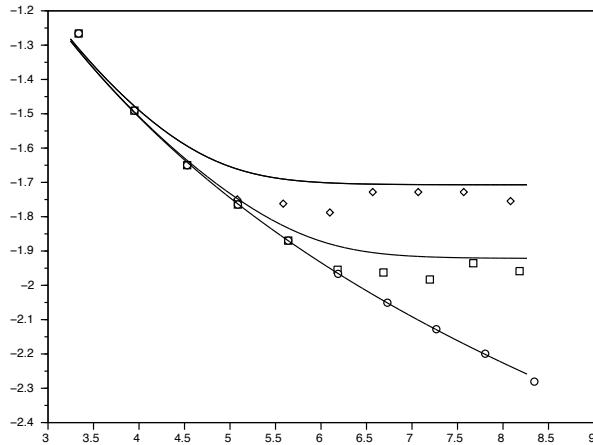


Figure 2: Moody chart ( $\log f$  vs.  $\log Re$ ) for different values of the relative roughness:  $\kappa = 0$  (circles),  $\kappa = 10^{-4}$  (squares),  $\kappa = 10^{-3}$  (diamonds). The lines are calculated using the (Colebrook, 1939) equation; symbols correspond to the Q3D calculations with  $C_\mu = 0.13$ .

### Flow modelling

The Reynolds-averaged Navier-Stokes equations read:

$$\frac{\partial \rho \mathbf{u}}{\partial t} + \nabla \cdot (\rho \mathbf{u} \mathbf{u}) = -\nabla p - \nabla \cdot \boldsymbol{\tau}, \quad (1)$$

where the Reynolds stress is modelled using the Boussinesq eddy viscosity assumption:

$$\boldsymbol{\tau} = \mu_T \left( \nabla \mathbf{u} + (\nabla \mathbf{u})^T - \frac{2}{3} (\nabla \cdot \mathbf{u}) \mathbf{I} \right) - \frac{2}{3} \rho k \mathbf{I}. \quad (2)$$

Being averaged along the horizontal chord Eq. (1) yields:

$$\frac{\partial \rho \bar{\mathbf{u}}}{\partial t} + \nabla \cdot (\rho \bar{\mathbf{u}} \bar{\mathbf{u}}) = -\nabla \bar{p} - \nabla \cdot \bar{\boldsymbol{\tau}} - \nabla \cdot (\rho \overline{\mathbf{u}' \mathbf{u}'}), \quad (3)$$

where  $\mathbf{u}' = \mathbf{u} - \bar{\mathbf{u}}$  and the last term in Eq. (3) is an additional Reynolds stress due to the averaging. Following the Boussinesq approach we model the combined Reynolds stress  $\bar{\boldsymbol{\tau}} + \rho \overline{\mathbf{u}' \mathbf{u}'}$  by Eq. (2), where equation for the turbulent viscosity reads:

$$\mu_T = C_\mu \rho \frac{k^2}{\varepsilon}. \quad (4)$$

In the present work we use the  $k - \varepsilon$  model in order to close Eqs. (3)-(4).

The standard version of the  $k - \varepsilon$  model assumes that  $C_\mu = 0.09$ ; due to the additional chord averaging  $C_\mu$  for the Q3D

model should be higher. In order to calibrate our model pressure drop in a pipe is been calculated with different values of  $C_\mu$ . The results are presented in Figure 2. One can see that the Q3D model is in a good agreement with the Moody chart over the entire range of Reynolds numbers and relative roughnesses.

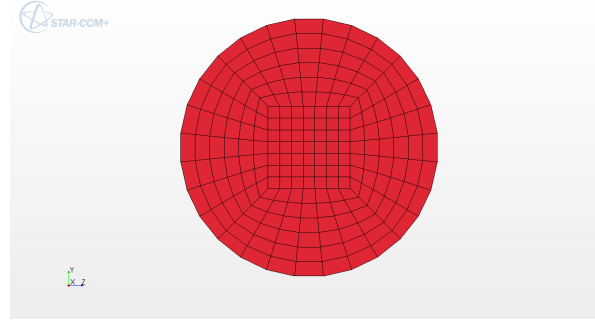


Figure 3: Fully 3D mesh.

## RESULTS AND DISCUSSION

### Hydrotransport

Transport of solids in horizontal pipelines is an important component of mineral processing industries (Karabelas, 1997; Eskin, 2012). The particles are suspended by the turbulent vortices against the gravity so the main force balance in the vertical direction is between the gravity force  $(\rho_S - \rho_L)\mathbf{g}$  and the turbulent dispersion force (TDF)  $\mathbf{F}_{TD}$ . Several functional forms for the turbulent dispersion force have been proposed in the past; in the present work we adopt the model derived by (Burns *et al.*, 2004) via Favre averaging of the Navier-Stokes equations for a two-phase flow:

$$\mathbf{F}_{TD} = 3D_T \frac{C_D}{d_p} |\mathbf{u}_R| \nabla (\ln \alpha_L - \ln \alpha_S). \quad (5)$$

Usually the turbulent dispersion coefficient is taken equal to the turbulent viscosity. This assumption is justified by the similarity between the turbulent mass and momentum transports. However, it was noted in the past that apparent diffusivity of the particles is higher than predicted. Taking the interphase slip into account (Eskin, 2012) proposed the following form for  $D_T$ :

$$D_T = \mu_T \left( 1 + \frac{\tau_s}{T_L} \right). \quad (6)$$

The particle relaxation time is estimated as

$$\frac{1}{\tau_s} = 3 \frac{\rho_L C_D}{\rho_S d_p} |\mathbf{u}_R| \quad (7)$$

and the Lagrangian time scale is given by the following formula:

$$T_L = C_\mu \frac{k}{\varepsilon}. \quad (8)$$

The calculations have been performed in Q3D and fully 3D modes. The 3D mesh is shown in Figure 3. Figure 4 shows distribution of  $165 \mu m$  sand particles in water under a moderate mean volume fraction of particles ( $\bar{\alpha}_S = 0.2$ ). The fully

3D calculations provide a justification for the chord averaging: as one can see, the level sets of  $\alpha_S$  are nearly horizontal.

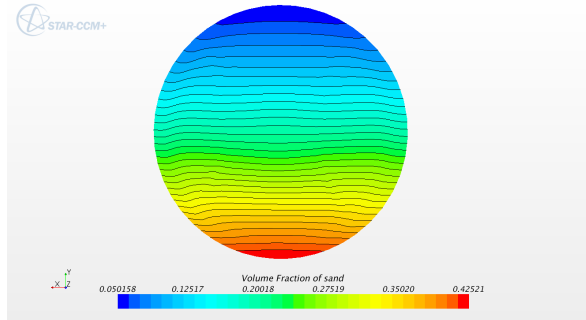


Figure 4: Volume fraction of sand in a horizontal pipeline; 3D mesh.

Distribution of the solid phase along the vertical centreline is shown in Fig. 5. Due to the TDF with the inertia correction (6) the results are in a good agreement with each other and with the experimental data (Karabelas, 1997).

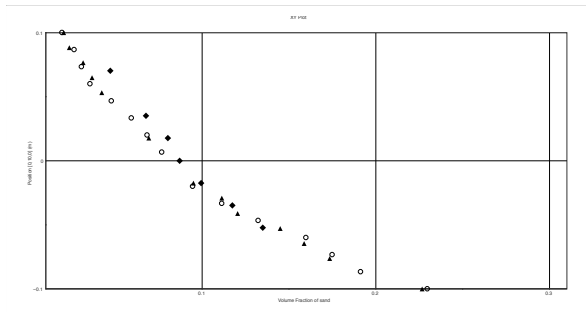


Figure 5: Distribution of sand (volume fraction vs. height) along a the centreplane of a horizontal pipeline; 3D mesh (circles), Q3D mesh (triangles), experimental data (diamonds).

### Slug flow

In order to assess the ability of the method to reproduce slug formation and evolution we performed a series of calculations under conditions described in (Ujang *et al.*, 2006). Gas-water flow in a horizontal 37m-long pipe with internal diameter 7.8cm was modelled by the volume of fluid (VoF) method on  $26 \times 6200$  Q3D mesh. Superficial gas velocity  $\mathbf{u}_L$  varies from  $0.22m/s$  to  $0.61m/s$ ; superficial gas velocity  $\mathbf{u}_G$  was set higher varying from  $2.27m/s$  to  $4.28m/s$ .

The flow is initialised with corresponding superficial velocity for each phase and volume fractions as it is shown in Fig. 6. Due to the unphysical initial conditions the flat interface is destroyed quickly by the Kelvin-Helmholtz instability as shown in Fig. 7. After a transient time a more physically plausible structure of slug flow is established, namely, there is a slug left behind a low volume fraction of water. As the gap between the wavy interface and the top of the pipe contracts, the gas accelerates and the slug overturns, so a typical slug

captures some amount of gas as it is shown in Fig. 8. The obtained structure of the volume fraction is characterised by a large bubbles of the gas trapped by the water; it is an artefact of the VoF method used. In the future a more advanced Eulerian multiphase method allowing for modelling of dispersed bubbly flows of will be used.

In order to detect the slugs we monitor the volume fraction of water at different cross sections of the pipe (Fig. 9). The slugs are characterised by a high volume fraction ( $\alpha_L \geq 0.8$ ). We manually count the number of peaks and the obtained slug frequency ( $0.3s^{-1}$ ) is in a good agreement with the experimental data by (Ujang *et al.*, 2006).

A better indication of the slugs dynamics can be obtained from the pressure distribution along the pipe as it is shown in Fig. 10. The pressure jump is just at the slug. The slug can be considered as a body with variable mass: there is water entering with low velocity  $\mathbf{u}_{in}$  (about  $3m/s$ ) and water left behind with velocity of the slug  $\mathbf{u}_{out}$  (about  $6m/s$ ). The momentum balance is

$$A\Delta P = \rho Q(\mathbf{u}_{in} - \mathbf{u}_{out}), \quad (9)$$

where  $A$  is the cross section area,  $Q$  is the volumetric flux through the slug,  $\Delta p$  is the pressure drop,  $\rho_L$  is density of water. The volumetric flux can be estimated as

$$Q = cA(\mathbf{u}_{in} - \mathbf{u}_{out}), \quad (10)$$

where  $c < 1$  is accounting for the fact that the water ahead of the slug occupies only a small (about 1/4) portion of the cross section. Therefore

$$\Delta p \approx c\rho(\mathbf{u}_{in} - \mathbf{u}_{out})^2 \quad (11)$$

and the obtained estimate is in a good agreement with the numerical results.

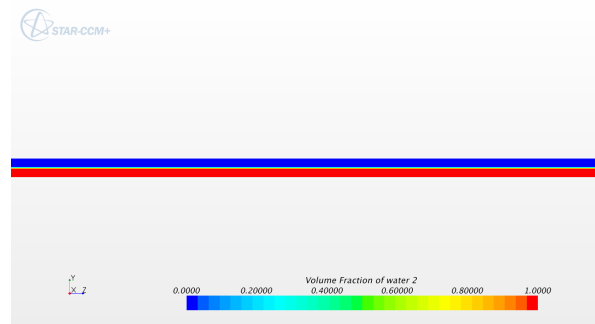


Figure 6: Slug flow: initial distribution of the volume fractions.

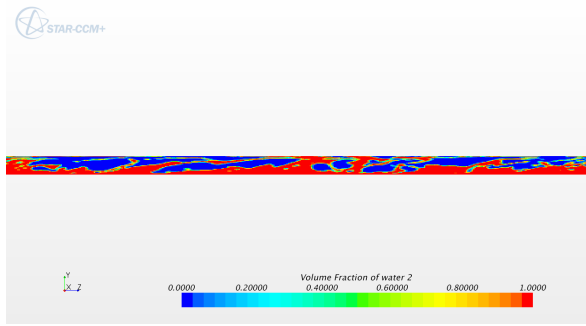


Figure 7: Slug flow: volume of fluid contour plot after 0.1s.

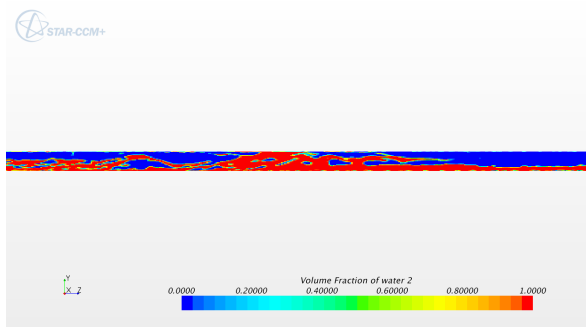


Figure 8: Slug profile after 100s;  $u_G = 4.28m/s$ ,  $u_L = 0.8/s$ .

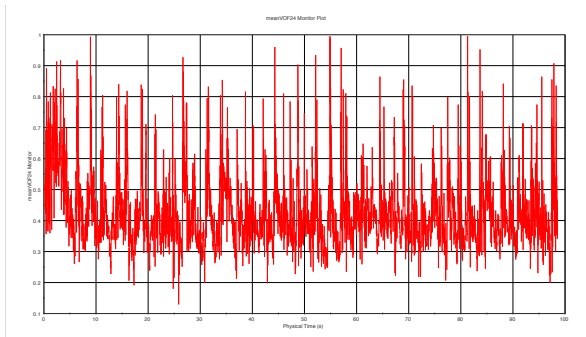


Figure 9: Cross-section averaged volume fraction as a function of time at 24m from the inlet;  $u_G = 4.28m/s$ ,  $u_L = 0.8/s$ .

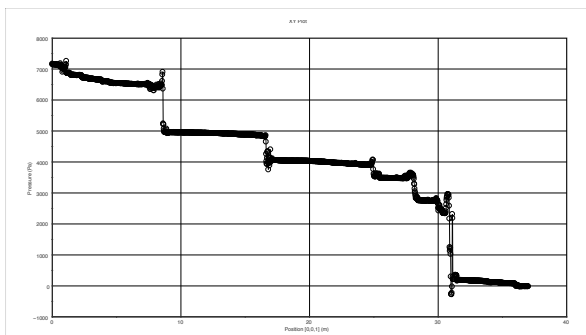


Figure 10: Pressure distribution along the pipe's centreline.

## CONCLUSION

The Q3D modelling of single and two-phase pipe flows can be done using the standard version of STAR-CCM+ code with a minimum modification of the standard simulation practice. Due to the numerous physical models (e.g., phase change, heat and mass transfer) available to a general user, it constitute a valuable alternative to development of a dedicated Q3D code.

## REFERENCES

BIBERG, D. (2007). "A mathematical model for two-phase stratified turbulent duct flow". *Journal of the ICE*, **11**, 1–48.

BURNS, A.D. *et al.* (2004). "The Favre averaged drag model for turbulent dispersion in Eulerian multi-phase flows". *5th International Conference on Multiphase Flows*. Yokohama, Japan.

COLEBROOK, C.F. (1939). "Turbulent flow in pipes". *Multiphase Sci. and Technology*, **19**, 133–156.

ESKIN, D. (2012). "A simple model of particle diffusivity in horizontal hydrotransport pipelines". *Chem. Eng. Sci.*, **12**, 84–94.

KARABELAS, A.J. (1997). "Vertical distribution of dilute suspensions in turbulent pipe flow". *AIChE Journal*, **23**, 426–434.

LAUX, H. *et al.* (2007). "Simulation of multiphase flows composed of large scale interfaces and dispersed fields". *6th International Conference on Multiphase Flows*. Leipzig, Germany.

UJANG, P.M. *et al.* (2006). "Slug initiation and evolution in two-phase horizontal flow". *International Journal of Multiphase Flow*, **32**, 527 – 552.